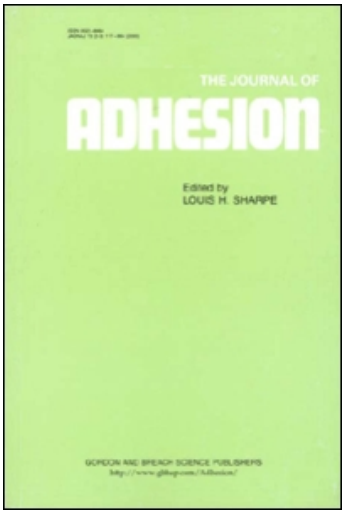

The Journal of Adhesion
Publication details, including instructions for authors and subscription information:
http://www.informaworld.com/smpp/title~content=t713453635

Adhesion in Solid Propellant Rocket Motors

Kai Frode Grythe[a]; Finn Knut Hansen[a]; Torbjørn Olsen[b]
[a] Department of Chemistry, University of Oslo, Oslo, Norway [b] Norwegian Defence Research Establishment, Kjeller, Norway

To cite this Article Grythe, Kai Frode , Hansen, Finn Knut and Olsen, Torbjørn(2007) 'Adhesion in Solid Propellant Rocket Motors', The Journal of Adhesion, 83: 3, 223 — 254
To link to this Article: DOI: 10.1080/00218460701239059
URL: http://dx.doi.org/10.1080/00218460701239059

The Journal of Adhesion, 83:223–254, 2007

ISSN: 0021-8464 print/1545-5823 online
DOI: 10.1080/00218460701239059

Taylor & Francis
Taylor & Francis Group

Adhesion in Solid Propellant Rocket Motors

Kai Frode Grythe
Finn Knut Hansen
Department of Chemistry, University of Oslo, Oslo, Norway

Torbjørn Olsen
Norwegian Defence Research Establishment, Kjeller, Norway

Plasma treatment of EPDM-based rocket motor insulation materials may change the peel strength between these materials and polyurethane polymers by a factor of 0.1 to 10. The matching of surface energies seems to be important for this adhesion process. The surface tension of the components was measured to between 30 and 50 mNm^{-1}. The total surface energy of the insulation could be increased from 27.2 mNm^{-1} to ca. 70 mNm^{-1} by the plasma process. Maximum peel strength could be obtained by a treatment of less than 1 min, whereas in most cases longer times gave lower values. In some cases very long treatment also gave good strength, probably due to a rougher surface structure. The rate of cure of the polymer was important for the adhesion process as lower rates of cure correlated with higher peel strengths, which can be explained by diffusion of the polymer's components into the insulation.

Keywords: Adhesion; Diffusion; Peel strength; Rocket propellants; Surface energy

NOMENCLATURE

AFM	Atomic force microscopy
BSE	Back-scattered electron
Bu-NENA	N-butyl-2-nitroethylnitramine
DBTDL	Dibutyltin dilaurate
DDI	Dimeryl diisocyanate
DOS	Dioctyl sebacate
EPDM	Ethylene propylene diene monomer

Received 14 August 2006; in final form 16 December 2006.
Address correspondence to Finn Knut Hansen, Department of Chemistry, University of Oslo, P.O. Box 1033 Blindern, 0315 Oslo, Norway. E-mail: f.k.hansen@kjemi.uio.no

GAP	Glycidyl azide polymer
HDPE	High-density polyethylene
HTPB	Hydroxyl-terminated polybutadiene
HTPE	Hydroxyl-terminated polyether
IPDI	Isophorone diisocyanate
MBCI	Methylenebis(4-cyclohexylisocyanate)
MDI	4,4′ diphenyl-methane diisocyanate
SE	Secondary electron
SEM	Scanning electron microscopy
XPS	X-ray photoelectron spectroscopy

INTRODUCTION

Solid propellant rocket motors are insulated thin-walled containers loaded with a propellant in which the most important ingredients are an oxidizer and a polymeric binder. The insulation material used to protect the motor casing against the high-temperature gas from the burning propellant is typically a particle-filled and fiber-reinforced EPDM. Adhesion in such a motor is a comprehensive problem. There are many interfaces where good adhesion is critical; perhaps the most important is the interface between the insulation material and the propellant.

According to adhesion theories [1], there are several mechanisms that may be involved in an adhesion process, some working together and some mutually exclusive. Adhesion can thus be achieved through physical adsorption, chemical bonding, interdiffusion, and mechanical interlocking and by electrostatic forces; the latter is probably less important in a polymer/polymer systems such as solid-propellant rocket motors. Mechanical interlocking can be achieved through the interface geometry but also by using rough surfaces. In a polymer/polymer system such as the rocket motor insulation/propellant interface, the interdiffusion of polymer chains between the phases is expected to be the most important mechanism for obtaining good adhesion; however, interdiffusion can also be a disadvantage in a reactive polymer system if one or more of the components diffuses across the interface and thus shifts the reactant ratio. In addition, this may pose a problem for the long-term stability of the bond, and it is therefore quite common to formulate the bonding system with a diffusion barrier [2,3].

To investigate the fundamental mechanisms of physical and chemical bonding and interdiffusion in a rocket motor, we have in previous work studied the diffusion properties in the different polymer phases [4,5]

and the surface energy and functional groups by plasma treatment of pure EPDM rubber surfaces [6]. In this article, we set out to investigate the practical adhesion in more real systems, and the objective is a utilization of earlier results and considerations in the understanding of adhesion in a real system. In the two earlier articles on diffusion, we measured self-diffusion coefficients in polyurethane formulations and mutual diffusion coefficients for materials typical of wall insulation and liners, respectively. Although self-diffusion and mutual diffusion coefficients cannot be directly compared, we think to have obtained basic information about the mobility of different components, especially diisocyanates, and how different solid matrices influence this mobility. In the article on surface modification [6], the effect of argon, oxygen, and nitrogen plasma treatment on pure solvent-cast EPDM rubber films was investigated by means of AFM, XPS, and surface energy measurements. Plasma treatment leads to increasing surface energies, from 25 to 70 mNm^{-1}, and treatment conditions influenced both the changes in surface energy and the stability. XPS analyses revealed that up to 20% oxygen can be easily incorporated in the surfaces and that variations can be controlled by the plasma conditions. Oxygen was mainly found as hydroxyl groups but also as carbonyl and carboxyl. The surface roughness increased generally with treatment time, and dramatic changes could be observed at longer times. At short times, surface energy changes were much faster than the changes in surface structure, showing that plasma treatment conditions can be utilized to tailor both surface energies and surface structure of EPDM rubber. By taking this information into account, in this work we have investigated the adhesion forces of different polymer materials with composition similar to liners and propellants to EPDM-based insulation materials modified by plasma treatment. The former materials will generally be denoted as "polymers" in this article.

The strength of an adhesive bond is directly proportional to the thermodynamic energies of adhesion [7], *i.e.*, the work of adhesion. Because the work of adhesion consists of the sum of dispersive and polar (or Lifshitz–van der Waals and acid–base) contributions, maximization of these interactions are among the fundamental guidelines in the improvement of adhesion in a given system [8]. The use of plasma treatment to increase the polar surface energy contributions and thus to improve the adhesion properties of polymers is a commonly used technique [9–16]. The surface is exposed to ions, electrons, molecular excited states, radicals, ultra violet (UV) and vacuum ultraviolet (VUV) radiation in a plasma [13,17], and the treatment has four major effects to a surface; cleaning, etching, cross-linking, and chemical modification. All of these effects may contribute to better bonding. One of the most

apparent results of plasma treatment is modified wettability of the surface, which is thought to be limited by the competition of chain scission (etching) and functional modification of the surface [13]. Generation of increased oxygen functionalities improves the wettability and can be achieved in oxygen-containing plasmas or by postplasma reactions [11]. Thus, plasma treatment increases the number of Lewis acid–base sites. In an acid–base perspective, oxygen-containing functionalities increase the strength of the Lewis acid–base interaction with water and other polar liquids. These groups give both an electron-donor character through the electron lone pair of oxygen and an electron-acceptor character through the active hydrogen linked to the electronegative oxygen atoms [8]. The stability of plasma-treated surfaces with time and as a function of environmental conditions is critical. All modified surfaces will be subject to aging, but by choosing the proper type of gas and the plasma-treatment conditions for the selected polymer, it is possible to minimize degradation and aging effects [11]. Some plasma-treated surfaces may remain stable for days and weeks [11,16,18,19], whereas others are much less stable [20]. Time is also an important factor in the analyses of plasma-treated surfaces, and the results may be strongly influenced by analysis times.

The modification of polymer surfaces by plasma treatment or by other means not only affects the energy of adhesion by modification of the surface polarity but also influences the miscibility of the polymers across the interface. It has been shown [21] that the bond strength at polymer/polymer interfaces is at its maximum when the surface energies of the two polymers are the same; surprisingly, a difference of only 1 mNm^{-1} significantly lowered the bond strength. Similar conclusions have also been obtained when considering the solubility parameters of the two polymers; the optimum bond strength is obtained when the solubility parameters match [22]. Now, the surface energy of a polymer is also connected to its solubility parameter(s), and therefore the latter has also with some success been used to predict the surface energy [23]. The fact that the matching of solubility parameters gives optimum bonding in a polymer/polymer system is readily understood from the energy of mixing and diffusion theory, and this becomes increasingly important for high-molecular-weight polymers because of the low entropy of mixing in such systems. Therefore, we believe that the effect of plasma modification of the low-energy surfaces to a large degree is to influence the interdiffusion of the higher-molecular-weight components, and in an isocyanate/polyol polyol composition this is mainly the polyol. The matching of solubility parameters and/or surface energies between the surface and the higher-energy polyol is therefore expected to be important; from these

considerations a very high surface energy after plasma treatment may even be a disadvantage. A question yet to be answered, however, is how far the interdiffusion has to go to achieve a good bond. It may be expected that this required distance will also be dependent on the surface geometry, *e.g.*, roughness.

In rubbers, as contrary to plastics, surface treatment may be more complicated because rubbers contain considerable amounts of additives that may be present in/on the surface, and also because rubber in general will be more prone to chain scission because of the presence of unsaturated bonds [24]. It is claimed [25] that there are very few effective pretreatments for additive-free EPDM, due to the low amount of double bonds. Plasma treatment of EPDM has been reported by a few investigators [25–29].

The surface energy of EPDM is quite low, and values ranging from 19 to 28 mNm^{-1} have been reported [29–32]. In a recent work, we have measured 22.2 mNm^{-1} for a pure solvent-cast EPDM surface [6]. In many articles, the EPDM quality is not specified, *e.g.*, whether it is a pure or filled EPDM rubber, the type and amount of diene, the content of additives, and the potential degree of cross-linking. This may be one reason for the differences in the reported surface energies, in addition to varying details in the method of measurement.

Mechanical testing of adhesive bonds is widely described in the literature [32–34], and many results are reported. It is generally accepted, however, that the magnitude of the measurements depend on the type of test, the test parameters, and the bonding system used. It may therefore be difficult to compare many of the reported values and thus also the effect of plasma treatments. Some results to be considered are those of Chin and Wightman [35], who report improvement in adhesion to HDPE from *ca.* 0.09 Nmm^{-1} to *ca.* 0.7 Nmm^{-1} after 1 min of oxygen plasma treatment, but that longer treatments had no significant effect on peel strength. Nihlstrand *et al.* [12] also reports increased peel strength from 0.007 to 2.3 Nmm^{-1} for polyurethane lacquer against a thermoplastic olefin surface after plasma.

EXPERIMENTAL

Chemicals

Isophorone diisocyanate (IPDI) was obtained from Degussa, Düsseldorf, Germany (trade name VESTANAT IPDI); dimeryl diisocyanate (DDI 1410) and dioctylsebacate (DOS) (Edenol 888) were obtained from Cognis, Loxstedt, Germany; metylenebis(4-cyclohexylisocyanate)

(MBCI or Desmodur W) was obtained from Bayer, Leverkusen, Germany; and 4,4′ diphenylmethane-4,4′ diisocyanate (MDI) was obtained from Sika, Switzerland (SikaForce-7010) and consists of a mixture of isomers and homologous components. Carbon Black Thermax was obtained from Cairn Chemicals Limited, Edinburgh, UK. Polyols glycidyl azide polymer (GAP) was obtained from SNPE, Paris, France; hydroxyl-terminated polyether (HTPE) from ATK, WV, USA; and hydroxyl-terminated polybutadiene (HTPB) (type R45 HT) from Elf Atochem, France. HTPE is a copolymer of tetrahydrofuran and polyethyleneglycol. N-Butyl-2-nitratoethylnitramine (Bu-NENA) was obtained from Dyno Defence, Norway, and dibutyltin dilaurate (DBTDL) was obtained from Sigma-Aldrich, Taufkirchen, Germany. All chemicals were used as received.

Sample Preparation

The insulation material consisted of EPDM rubber, cross-linked and filled with fibers, flame retardants, and other substances. The exact composition is not disclosed by the manufacturer. The material is a typical insulating material used to protect the rocket motor case from the high-temperature gas. The rubber composite is delivered in a B-stage by ATK, Rocket Center, WV, USA, and manufactured into sheets by Nammo Raufoss, Raufoss, Norway. Prior to analysis and plasma treatment, the samples were cleaned with ethanol and dried at 60°C for 5 h. The polymers used, described in Table 1, were mixed together by hand and evacuated to remove air bubbles. All peel samples were prepared no later than 40 min after mixing of the polymer. The peel samples were cured at 60°C for 72 h (HTPB polymer cured 168 h), under a pressure of *ca*. 10 gcm^{-2}.

TABLE 1 Details of the Composition of the Polyurethane Polymers (C/P is the Molar Ratio between Isocyanate and Hydroxyl Groups

Polymer	Polyol	Curing agent	C/P	DBTDL (ppm, w/w)	Carbon black (%, w/w)
GAP-F	GAP	MDI	1.2	53.4	28.9
GAP-S	GAP	MDI	1.2	0	28.9
HTPE-F	HTPE	MDI	1.2	7.5	28.9
HTPE-M	HTPE	MDI	1.2	2.5	28.9
HTPE-S	HTPE	MDI	1.2	0	28.9
HTPB	HTPB	IPDI	2	*	20

*Less than 1% triphenyl bismuth, maleic anhydride, and MgO.

The plasma chamber (Plasma Science, CA, USA, PS0150E) is equipped with a 500-W RF generator and a 13.56-MHz high-frequency power supply. RF power is applied to two side electrodes, and the gas flow is in the direction of front to back. Insulating materials are used to reduce wall/electrode interactions, thus giving uniform plasma throughout the reaction chamber. The chamber has three mass flow controllers, allowing a gas flow on the order of 5–500 sscm (standard cubic centimeters per minute). The samples were placed in the middle of the chamber, and before and after each treatment the chamber was evacuated to a base pressure of 0.025 torr. After the treatment, air was let into the chamber until atmospheric pressure was reached. All samples were stored dry in closed dishes/plastic bags at room temperature after plasma treatment.

The main plasma-treatment parameters are the time of treatment, the type of gas, the gas flow rate, and the power input. Three different gases have been used: oxygen, nitrogen, and argon. The treatment time, the power input, and the gas flow rate were chosen from the results of our earlier work [6]. For oxygen and nitrogen plasmas, gas flow rate and power input of 100 sscm and 500 W, respectively, were used, whereas for argon plasma the gas flow rate and power input were 450 sscm and 250 W, respectively.

Surface Tension Measurements

Surface tension was measured by two different methods, one using a manual Du Noüy ring tensiometer (Krüss, Hamburg, Germany) and the second with a drop-shape analysis instrument (ramé-hart Instrument Co., Mountain Lakes, NJ, USA, with the DROPimage® software). All measurements were carried out at room temperature. All glass equipment was thoroughly cleaned in chromic sulfuric acid and rinsed in distilled water prior to use. The platinum ring was washed in ethanol and flamed before each measurement. Because some of the liquids measured were quite viscous, care was taken to ensure equilibrium conditions. In the ring tensiometer, all measurements were tested for equilibrium by keeping the tension at a value *ca*. 0.5 mNm^{-1} lower than the final surface tension for at least 15–20 min without breaking the surface. All reported values are an average of at least three measurements, with a deviation of less than 0.5 mNm^{-1}. The surface tensions measured by drop shape, were obtained by analyzing images of a sessile drop on a specially made sample holder cleaned in chromic sulfuric acid. The sample holder was made of a Teflon® bar with a drilled depression in the middle for the drop. For each sample, the reported value is an average of

10 measurements, with 30 s between each measurement. The surface tension is calculated from the equation

$$\gamma = \frac{\Delta\rho g R_0^2}{\beta}, \tag{1}$$

where $\Delta\rho$ is the mass density difference between the drop and the surrounding medium, g is the acceleration of gravity, R_0 is the radius of curvature at the drop apex, and β is a shape factor [36]. The interfacial tensions were measured in the same way for sessile or pendant drops. Pendant drops hanging from a thin glass capillary were used when the density of the drop was higher than that of the bulk liquid. In the opposite case, sessile drops were measured on the Teflon® sample holder. The densities of the liquids were measured by pychnometry.

Contact Angles and Surface Energy Measurements

Advancing contact angles were measured with an automated contact-angle goniometer (Model 200, ramé-hart Instruments Co., Mt. Lakes, NJ, USA), including an automated dispenser and the DROPimage® computer program. The contact angles were measured by increasing the drop volume in steps of 1 μl and measuring the resulting angles on both sides of the drop after 1 s. For each liquid, an average of 15 measurements, distributed between three different drops, were recorded, and the exact number was determined by the reproducibility of the measurements. Also, because we earlier found heterogeneities in the EPDM surface, contact angles were measured on three to seven different samples, all separately plasma treated. Thus, 100–300 measurements on each side of the drop for each plasma treatment gave a standard deviation of $\pm 1\%$.

To calculate the surface energy from contact angles, different methods are commonly used, but opinions vary widely on the suitability of several of these, and they also tend to give different results. One of the most recognized methods is Fowkes's theory, where the surface energy is split into a dispersive and a polar component, and the geometric mean of the dispersive components is used to calculate the work of adhesion. In the so-called extended Fowkes's theory [37–39], the geometric mean of the polar components is added, so that the expression for the work of adhesion is

$$W_{12}^{a} = 2(\gamma_2^{d}\gamma_1^{d})^{0.5} + 2(\gamma_2^{p}\gamma_1^{p})^{0.5} = \gamma_1(1 + \cos\theta). \tag{2}$$

Here, indices 1 and 2 are used for the liquid and solid, respectively, and θ is the contact angle. Solving this equation for a set of two liquids

yields a polar and a dispersive surface energy component. Instead of the geometric mean, the use of a harmonic mean for the work of adhesion has also been argued for [32], especially for polymeric surfaces. In that case, Equation (2) becomes

$$W_{12}^{a} = \frac{4{\gamma_1}^{d}{\gamma_2}^{d}}{{\gamma_1}^{d} + {\gamma_2}^{d}} + \frac{4{\gamma_1}^{p}{\gamma_2}^{p}}{{\gamma_1}^{p} + {\gamma_2}^{p}} = \gamma_1(1 + \cos\theta). \tag{3}$$

These methods are simple, but it is often observed that the polar component of the surface energy depends on the choice of liquids, and therefore, it is not an intrinsic property of the solid surface [40]. The method is referred to as the *two-liquid* method. In our measurements, a geometric mean appears to give generally more reproducible and probable results and is used in all the calculations. The calculation tools are built into the DROPimage program. Surface energy parameters for the liquids that are used in this work [41] are given in Table 2.

The interfacial tension between two liquids can be calculated from the surface tensions of the separate liquids and the work of adhesion, W_{12}, between them by

$$\gamma_{12} = \gamma_1 + \gamma_2 - W_{12}. \tag{4}$$

In addition, each surface tension consists of the sum of the dispersive and polar components, so that

$$\gamma_1 = \gamma_1^{d} + \gamma_1^{p}, \qquad \gamma_2 = \gamma_2^{d} + \gamma_2^{p}. \tag{5}$$

By using a geometrical mean for both the dispersive and polar components, the work of adhesion can be expressed by

$$W_{12} = W_{12}^{d} + W_{12}^{p} = 2\sqrt{\gamma_1^{d}\gamma_2^{d}} + 2\sqrt{\gamma_1^{p}\gamma_2^{p}}. \tag{6}$$

Thus, if the dispersive and polar components are known for one liquid, they may be calculated for another liquid by measuring the surface tension of the second liquid and the interfacial tension between the two liquids. However, it should be noticed that this way of calculating

TABLE 2 Surface Energy Parameters for the Liquids Used (Values in mNm^{-1})

Liquid	γ	$\gamma^{d} = \gamma^{LW}$	γ^{p}
Water	72.75	21.75	51.00
Diiodomethane	50.80	50.80	0

the interfacial tension is somewhat approximate and assumes that Equation (6) is correct. It also assumes that the liquids are mutually insoluble, which is also not always the case. Therefore, it cannot be expected that interfacial tension calculated by this method will be exactly equal to experimental values, or, the other way around, that polar and dispersive components calculated from these equations are universal constants, completely independent of the liquid/liquid combination. It is possible to improve the general feasibility of the results by using several liquid/liquid pairs and taking the average between the results.

Scanning Electron Microscopy

A scanning electron microscope (SEM) has its great strength in giving a wide depth of view, compared with light microscopy and is, therefore, widely used to study the topography and morphology of surfaces. A narrow electron beam scans the surface, and both secondary electron emission (SE) and back-scattered-electron Emission (BSE) are registered. A Hitachi S-3600N SEM (Hitachi, Tokyo, Japan) was used here. All samples were coated with gold, and the pictures were generated in high-vacuum mode. Both SE and BSE pictures were used, but generally BSE gave the best contrast. To prepare samples for SEM, 300-μm-thick slices were cut across the bonding surface with the help of a microtome (Microm International, Walldorf, Germany, HM 355S).

Mechanical Testing of Bonding

Peel tests are a common way of assessing bonding strength [32,34]. Most often the peel force will vary either randomly or in a stick–slip pattern with regular peaks; the variations in the sample being caused by occasional defects. All measurements were so-called T-peel tests, described in ASTM D 1876. Two pieces of insulating material were glued together with the specific polymer and tested as shown in Figure 1. The sample size and the peel velocity used were not in agreement with ASTM D 1876 but were considered more suitable to our samples. From approximately 50-mm-wide-samples, (37 ± 2)-mm-wide samples were cut, with a precision of 0.1 mm. In the calculation, the precise width is used for each sample. The samples were peeled at a rate of 50 mm/min. The reported values are in most cases the average of two samples, but in some cases up to four samples were tested, and in a very few cases only one sample was

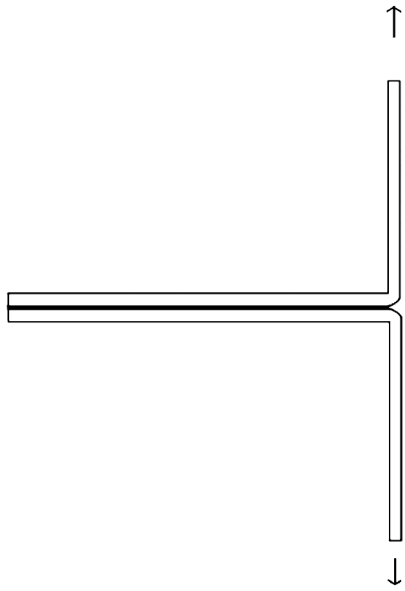

FIGURE 1 Principle for T-peel test.

tested. When multiple samples were tested, error bars are depicted in the data plots.

THEORETICAL CONSIDERATIONS

In polymer–polymer adhesion, the primary adhesion mechanism is expected to be interdiffusion of polymer chains across the interface. It is well known that incompatible polymers also usually have low mutual adhesion. As mentioned in the introduction, it has also been shown that adhesion is optimal when the surface energy (surface tension) of the two polymers is the same. In this article, we consider both the effect of diffusion and the effect of interfacial tension in a real polymer/polymer system. We have shown earlier [4] that the different species in polyurethane polymers as utilized in several of the components in a rocket motor have widely varying diffusion coefficients, both dependent on molecular weight and polarity of the molecule itself and on its surroundings. Among the diisocyanates used as curing agents in rocket motor liners and propellants, the diffusion coefficient can vary between $6 \times 10^{-11}\,\mathrm{m^2 s^{-1}}$ (self-diffusion coefficient of pure IPDI) down to very low (immeasurable) values, $< 10^{-16}\,\mathrm{m^2 s^{-1}}$. A typical value for MDI in EPDM insulation is

ca. $2 \times 10^{-14}\,m^2s^{-1}$, whereas in a cured polyurethane copolymer it can be 10–100 times higher. The diffusion coefficients of the polyols in a noncured polymer mix can be quite high, whereas they are nonmeasurable in the EPDM insulation. Therefore, to evaluate the effect of diffusion on the adhesion, the components themselves, the molar ratio, and the rate of cure all must be taken into account. The rate of cure may be important because a slower rate of cure will keep the unreacted isocyanate in contact with the insulation for a longer time, and thus make more diffusion into the insulation possible. On the other hand, as long as the polyol does not penetrate the insulation, the effect of this diffusion may be questionable. However, diffusion of isocyanate may open up the EPDM network to make room for simultaneous diffusion also of the polyol. This secondary diffusion process may also be strongly dependent on the solubility of the polyol in the surface layer, which is thought to be influenced by the plasma treatment. Diffusion of the isocyanates into the insulation may also have a secondary effect because the molar ratio between diisocyanate and polyol in the polymer is changed, which may influence the molecular weight of the polymer. A shortage, as well as an excess, of diisocyanate will give a lower molecular weight, and a shortage will also give hydroxyl-terminated polymers with a higher surface energy and less reactivity against, for instance, other components and even the insulation itself.

To evaluate the effect of the rate of cure, we can use the diffusion coefficients from Grythe, Hansen, and Walderhaug [4] and Grythe and Hansen [5], where we measured the self-diffusion coefficients for the same curing agents and polyols that have been used in the present work, at different mixing ratios. We can use these data to evaluate the depth of penetration of the components into the insulation, assuming this rate is correlated to adhesion. Each component will have two different diffusion coefficients, one in the polymer and one in the insulation. In a reacting system, the diffusion coefficients will decrease with time, possibly to zero, dependent on molar ratios, *etc*.

In a first model, constant diffusion coefficients (no reaction) can be assumed. In this system, the diffusion across the interface will create concentration gradients on both sides. With no accumulation at the interface, Fick's first law says

$$D_1 \frac{dc_1}{dx} = D_2 \frac{dc_2}{dx}, \tag{7}$$

where x is distance, c_1 and c_2 are concentrations, and D_1 and D_2 the diffusion coefficients in the phases 1 and 2, respectively. Because the

solubility of the diffusing species can be different in the two phases, the ratio between the equilibrium concentrations is not 1, and this gives a discontinuity in the concentration at the interface with

$$\frac{c_1}{c_2} = k. \tag{8}$$

Here k is the equilibrium constant between the solubility in the two phases. The solution of the concentration as a function of time and distance also involves the solution of Fick's second law and is not detailed here. The interested reader is referred to the cited literature. If the initial conditions are a concentration of C_0 of the diffusing specie in phase 1 and 0 in phase 2, the solution for c_1 and c_2 as a function of time, t, is [42]

$$c_1 = \frac{C_0}{1 + k\sqrt{D_2/D_1}}\left[1 + k\sqrt{D_2/D_1}\,\mathrm{erf}\frac{x}{2\sqrt{D_1 t}}\right] \tag{9}$$

$$c_2 = \frac{kC_0}{1 + k\sqrt{D_2/D_1}}\,\mathrm{erfc}\frac{|x|}{2\sqrt{D_2 t}} \tag{10}$$

where erf is the error function and erfc the complimentary error function, $\mathrm{erfc}(y) = 1 - \mathrm{erf}(y)$. They may be easily evaluated (*e.g.*, by MS Excel). These equations can be used to simulate concentration profiles. For the diffusion coefficients on the polymer side, self-diffusion coefficients from Grythe, Hansen, and Walderhaug [4] can be used with some care, as the self-diffusion coefficients are not the same as the mutual diffusion coefficients. The mutual diffusion coefficient for the binary mixture, D_{12}, is connected to the separate self-diffusion coefficients, and may in principle be calculated from these, but this is not a straightforward procedure. Many different expressions have been proposed, one of the simplest being [43]

$$D_{12} = B_2^x(x_2 D_1 + x_1 D_2), \tag{11}$$

where

$$B_2^x = \frac{1}{RT}\left(\frac{\partial \mu_2}{\partial \ln x_2}\right)_{T,p} = 1 + \left(\frac{\partial \ln f_2}{\partial \ln x_2}\right)_{T,p} \tag{12}$$

is the thermodynamic factor. Here D_i are the individual self-diffusion coefficients, x_i is the mol fractions of each component, μ_2 is the

chemical potential, and f_2 is the rational activity coefficient of component 2. This equation is also known as the Darken equation and has been widely used, but it has some limitations. However, it does represent the limiting behavior expected for the mutual diffusion coefficient at each end of the concentration scale. When either x_1 or x_2 approaches zero, $B_2^x \rightarrow 1$, and D_{12} is then given by the extrapolated self-diffusion coefficient of the respective components at infinite dilution in the other component. For a polymeric system, B_2^x might be calculated by the Flory–Huggins theory, but missing the interaction parameter in this theory, we have not attempted this. In addition, the linear dependence of D_{12} on B_2^x has also been debated, so there is a question of the justification of such a procedure. Because a normal mix for a poly(urethane) is usually made at an approximately equimolar ratio ($x_1 = x_2 = 0.5$), we may anticipate that in the cases where $D_1 \gg D_2$, the value of D_{12} will be most close to D_1.

RESULTS AND DISCUSSION

Surface Tension of the Components

In Table 3, the measured surface tensions are shown for some common polyols, curing agents, and plasticizers used in the rocket motor industry. These values are of interest because they give information about the possible need for surface modification of the insulation surface and the expected level of modification. The surface tensions range

TABLE 3 Surface Tensions Measured by a Ring Tensiometer; Some Values Also by Drop-Shape Analysis (Marked^{ds})

Substance	γ (mNm^{-1})	Density g/cm^3	γ^d (mNm^{-1})	γ^p (mNm^{-1})
MDI	30.5	1.239	17.3	13.2
DDI	36.2	0.924	34.1	2.2
IPDI	37.2	1.061	32.2	5
MBCI	42.9	1.071	41.5	1.5
HTPB	39.1, 36.2^{ds}	0.901	$\approx$39.1	$\approx$0
HTPE	41.9, 42.2^{ds}	1.049	30.8	11.1
GAP	50.3, 51.6^{ds}	1.290	33.4	16.9
DOS	32.7	0.913	32.7	$\sim$0
Bu-NENA	39.2	1.227	29.0	10.2
SiOil	22.4	0.968	21.7	0.7

Note. Dispersive and polar surface tension component are calculated from Equations (4) and (5) and the measured density of the liquids.

TABLE 4 Interfacial Tension Measured by Drop-Shape Analysis; Some Values Also by a Ring Tensiometer (Marked[r])

System (drop/bulk)	γ_{12} (mNm^{-1})
Water/SiOil	39.6
SiOil/DDI	2.5
IPDI/SiOil	3.0, 3.0[r]
MDI/SiOil	8.1, 8.0[r]
MBCI/SiOil	3.4
GAP/SiOil	12
HTPE/SiOil	ca 7
Bunena/SiOil	6.1
DOS/Water	23.3[r]
SiOil/DOS	0.5, 0.5[r]

from 30.5 to 50.3 mNm^{-1}. Silicone oil (SiOil) is included in this table, because it is used to measure the interfacial tension in Table 4.

To split the surface tension into its polar and dispersive parts, interfacial tensions between the different components and SiOil were measured. The automatic drop-shape method was preferred because of its efficiency and the need for lower amounts of substances, but the ring tensiometer gave very similar results, as seen in Table 4. SiOil was used as the preferred contact medium for the measurement of interfacial tensions, because of its density and inertness against the other chemicals. By measuring the interfacial tension between two immiscible liquids, it is possible to calculate γ^d and γ^p for a liquid as described previously. The surface tension components for SiOil were calculated from measurements against water, because the components of water are well known. All results are shown in Table 3. When it comes to polarity, the measured liquids can be divided into three regimes. First, the liquids that can be considered nonpolar include DOS and HTPB. Second, MBCI, DDI, and IPDI have a polar component around 2–5 mNm^{-1}, and last, MDI, BuNENA, HTPB, and GAP have polar components higher than 10 mNm^{-1}. The liquids can also be divided into three groups by their dispersive component: MDI has less than 20 mNm^{-1}; Bu-NENA, DOS, GAP, HTPE, IPDI and DDI around 30 mNm^{-1}, and HTPB and MBCI around 40 mNm^{-1}.

As the parameters of the plasma treatments can be chosen within wider limits than used in this work, it may be possible that by choosing other parameter combinations the surface energies of the polymers outside of those values reported in this article can be obtained. Thus, it may be possible that further improvements in the peel strength can be achieved.

Contact Angles and Surface Energies of EPDM Insulation

The contact angles of water and diiodomethane after plasma treatments of the R1100 EPDM insulation are plotted in Figure 2 as a function of the treatment time. Results for the three different plasma gases (oxygen, nitrogen, and argon) are shown in Figures 2A, 2B, and 2C, respectively. It is apparent that the contact angles change dramatically once the samples are plasma treated, in the same way as observed earlier for the pure EPDM surfaces [6]. Before treatment, water and diiodomethane had contact angles of 97° and 65°, respectively. The greater part of the change takes place during the first 30–60 s after the samples are exposed to the plasma. For oxygen plasma, a minimum in the contact angles and surface energies were observed after 30 s; thereafter a minor increase can be seen. The minimum is 57° for water and 54° for diiodomethane. For nitrogen and argon plasma treatments, there are no minima, but there is a distinct change after 30–60 s, where afterward the decrease is much slower. Argon treatment seems to be the most efficient, giving contact angles of 32° for water and 38° for diiodomethane after 6 min of treatment. For nitrogen plasma, the contact angles are 40° and 47° for water and diiodomethane, respectively, after 6 min of treatment. Oxygen was clearly the less efficient treatment. The change in the contact angle of water was higher than the change for diiodomethane. The trend is also in agreement with what we have found in the earlier work on a pure EPDM film [6].

Figure 3A shows the total, dispersive, and the polar surface energy components, calculated by the two-liquid method, Equation (2). An untreated EPDM sample has a total surface energy of 27.2 mNm^{-1}, with a polar component of 1.4 mNm^{-1}. After 30 s of plasma treatment, the total surface energy was *ca.* 50 mNm^{-1} for argon, nitrogen, and oxygen treatment. After 2 min, the total surface energy was *ca.* 47 mNm^{-1} for the oxygen treatment, whereas for nitrogen and argon treatments it had increased to almost 60 mNm^{-1}. After 6 min, the oxygen-treated sample had a total surface energy of 43 mNm^{-1}, the nitrogen-treated sample 62 mNm^{-1}, and the argon-treated sample 68 mNm^{-1}. Most of the change in the surface energy is due to the change in the polar component, but an increase in the dispersive component of 5–10 mNm^{-1} can also be seen. Again, compared with our results with pure EPDM, the trend is much the same, but the total surface energy change is a bit lower and the initial change is slower. Both observations are probably explained by the more composite nature of the commercial EPDM rubber surfaces. The content of fibers and inorganic additives make the surface more inert against attack

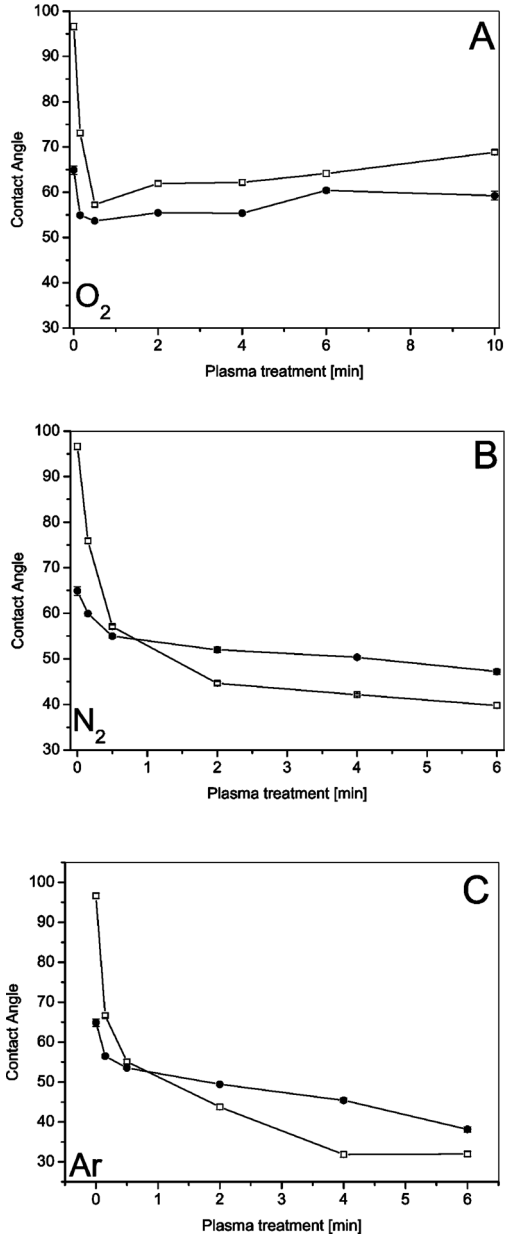

FIGURE 2 Contact angles of water (□) and diiodomethane (●) on EPDM surfaces treated by oxygen (A), nitrogen (B), and argon (C) plasma.

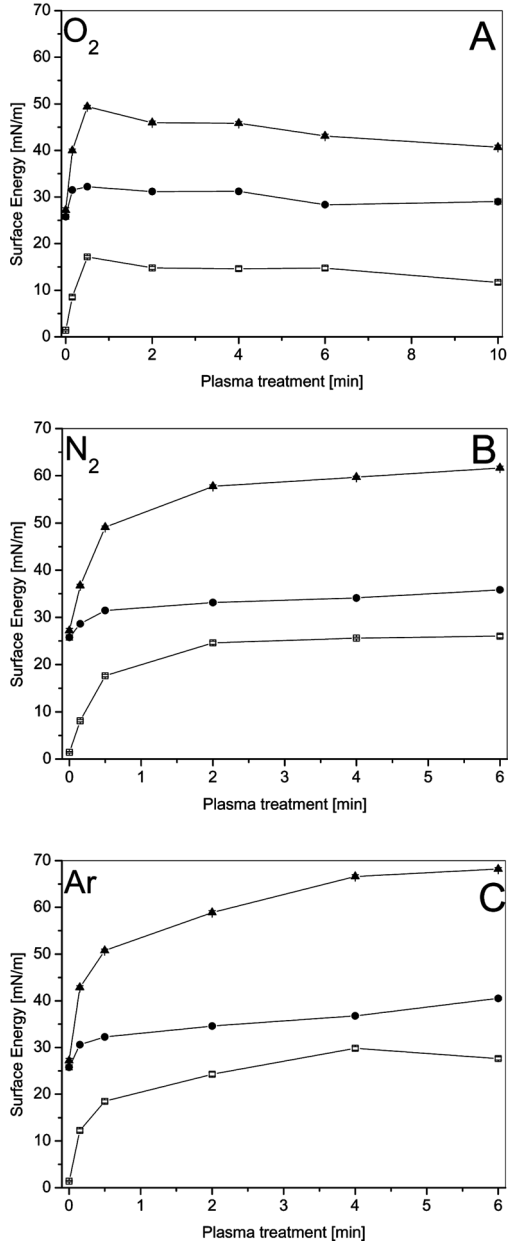

FIGURE 3 Polar (□), dispersive (●), and total (▲) surface energy of EPDM surfaces treated by oxygen (A), nitrogen (B), and argon (C) plasma.

of the radicals in the plasma gas, but it is satisfactory to observe that the main effects and trends are the same. The results from the pure EPDM surfaces may therefore be used as indicators for what may be expected from commercial surfaces.

Mechanical Testing of Bonding

The production of samples for mechanical testing is very time consuming and therefore only a selected number of tests could be conducted. The plasma treatment conditions investigated were the same as in the surface energy measurements, but for each gas only three different treatment times were used: short, medium, and long treatment times of 0.15 (or 0.5), 2 and 6 min, respectively. The choice of polymer ("adhesive") for the bonding is a key parameter for obtaining quantitative information from these tests. If the polymer adhesion to the EPDM insulation surfaces is very high, one can expect to see cohesive failure in either the insulation or the polymer itself. Such a failure gives no quantitative information on the adhesive strength, only that it is at least as good as the cohesive strength of the insulation. On the other hand, if the adhesive strength between polymer and the insulation is very low, differences in the adhesive strengths can be more difficult to measure. It is also important that the flexibility of the polymer is at least as high as the insulation itself; otherwise this will affect the 180° bending necessary for the T-peel test. We have also found that the rate of cure of the polymer is crucial for the peel strength, probably because of the diffusion of species from the polymer into the insulation. With a slower rate of cure, the low molecular species will be present longer in the system and have a chance to diffuse into the other phase. According to the diffusion theory of adhesion, this should have a positive effect on the adhesion strength. On the other side, if the diffusion rates of the components of the polymer into the insulation are different, *e.g.* if the diisocyanate is diffusing faster that the polyol, this will affect the molar ratio between the monomers and may thus change the polymer's molecular weight. If the monomer molar ratio is formulated to maximize the molecular weight, a change in the ratio will lower the molecular weight and thus the strength.

The results from the peel testes are shown in Figures 4–6. In Figure 4A, the results for the GAP-F polymer are seen. The uncertainties involved in some of the measurements are quite large, but still some trends are clear. For oxygen plasma treatment, the peel strength is increasing with the plasma treatment time, from 0.18 Nmm^{-1} for the 30-s treatment to 0.55 Nmm^{-1} for the 10-min treatment. On the other hand, nitrogen plasma treatment shows a large improvement

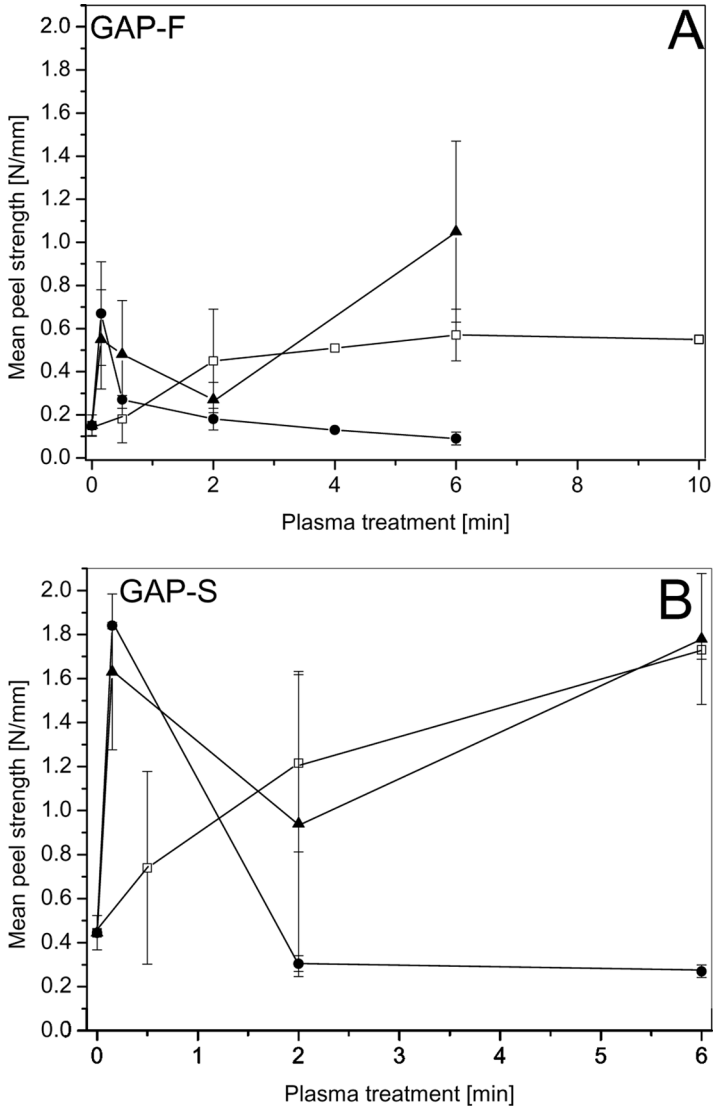

FIGURE 4 Mean peel strength for oxygen- (□), nitrogen- (●), and argon- (▲) plasma-treated EPDM using GAP-F (A) and GAP-S (B) polymer.

in the peel strength after only 9 s of treatment, but longer treatment times again give decreasing peel strengths; after 6 min of plasma treatment it is down to almost the level of the untreated sample. For argon plasma treatment, the uncertainties in the peel strengths are

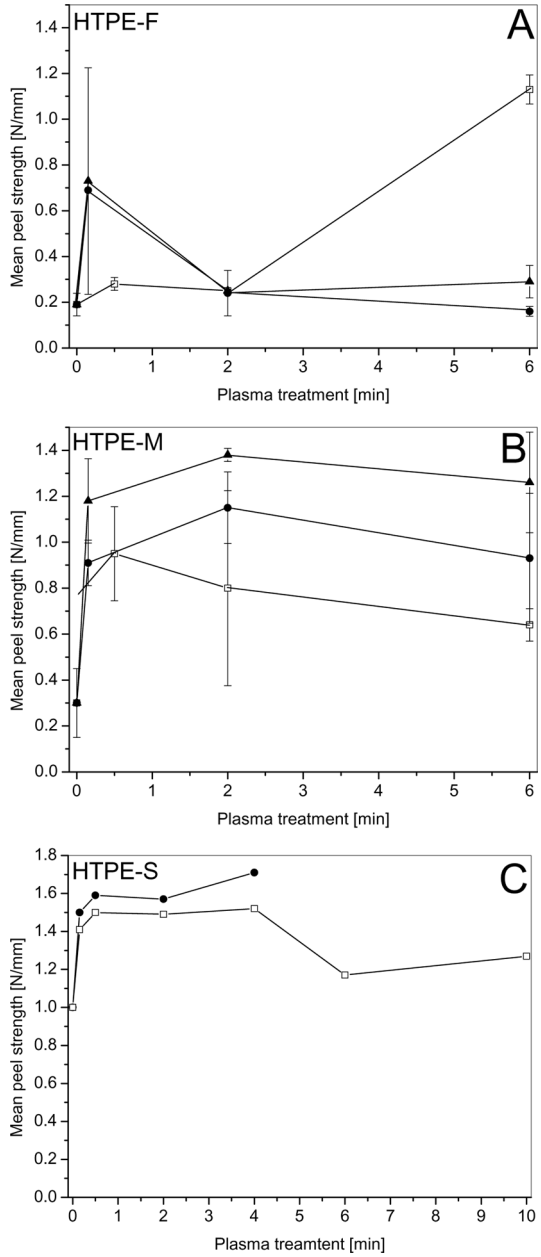

FIGURE 5 Mean peel strength for oxygen- (□), nitrogen- (●) and argon- (▲) plasma-treated EPDM using HTPE-F (A), HTPE-M (B), and HTPE-S (C) polymer.

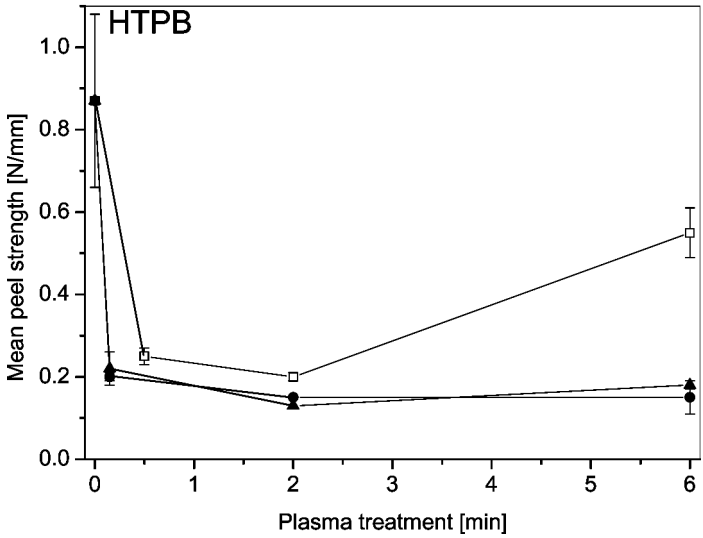

FIGURE 6 Mean peel strength for oxygen- (□), nitrogen- (●) and argon- (▲) plasma-treated EPDM using HTPB polymer.

large, but the results are generally the same as for oxygen plasma treatments.

To compare peel strength with surface energies presented in Figure 3, we observe from Figure 3A that oxygen plasma gives quite stable surface energies, with a total energy of a little less than 50 mNm^{-1} and a polar energy of 17 mNm^{-1} after *ca*. 30 s of treatment. After a few minutes, the total surface energy is $\approx$45 mNm^{-1} with the polar component $\approx$15 mNm^{-1}. The peel force is approximately constant after *ca*. 2 min (this time is somewhat uncertain). For both argon and nitrogen, the peel force has a maximum after just a few seconds of exposure, before a significant decrease. If we compare this with the surface energy measurements, we see that the total surface energy is 35–46 mNm^{-1} (the polar component 8–12 mNm^{-1}) after a few seconds of plasma exposure and increases to a total of 55–70 mNm^{-1} (polar component 25–30 mNm^{-1}) after a few minutes of exposure. This surface energy is much higher than the surface energy (surface tension) of the polymer, and the large mismatch may be the reason for the decreasing peel strength.

If we compare the surface energies of the surface and the polymer, there is a question of the influence of the different components of the polymer mixture and also how this is changing with time when the polymer is cured and even when the composition changes by preferred

diffusion of one of the components, as discussed previously. Because the diffusion coefficient of the diisocyanate is much higher that that of the polyol, it will probably be the penetration of the diisocyanates into the surface that has the strongest influence on adhesion, even if the diffusion of the polyol also plays a role. So, the influence of the surface energies of the individual components may change with time, but after a certain reaction time a copolymer will be formed, and then the surface energy of the whole polymer should be important. The surface energy, γ_{AB}, of the mixture of components A and B could be calculated from the individual surface tensions, γ_A and γ_B, respectively, but this would require more information about the degree of interaction between the components. Only in an ideal mixture will the surface tension contributions be additive, but it may be safe to assume that the surface tension of the mixture is somewhere between those of the individual components. Additionally, the insulation interface may influence the relative composition of the interface of the mixture, so the interfacial tension of the mixture and the insulation cannot be directly computed from the surface tension(s). Therefore, we will principally compare the surface energy of the insulation with the surface energies of the individual components.

The total surface energy (surface tension) of GAP is $50.3\,\mathrm{mNm}^{-1}$ (polar component of $16.9\,\mathrm{mNm}^{-1}$) and that of MDI is $30.5\,\mathrm{mNm}^{-1}$ (polar component $13.2\,\mathrm{mNm}^{-1}$). The high peel forces observed for all oxygen plasma treatments may therefore be explained well with the matching of surface energies, because the surface energies are approximately the same for the EPDM insulation surfaces as for the GAP-F polymer. For the nitrogen and argon plasma treatments, the surface energies can also explain the maxima in peel strength observed after a few seconds of plasma treatment, as the surface energies then are similar. Longer treatment times give much higher polar energies of the EPDM surface, considerably higher than of the GAP polymer, and the peel force decreases. However, the picture is not unambiguous, as 6 min of argon plasma treatment gives a very high peel force. There are also large uncertainties in the latter value, and other parameters such as the increased roughness in the sample surface after long argon plasma treatments [6] may complicate the picture. It may well be that the increased roughness again favors adhesion, so the total effect of the plasma treatment is not necessarily only on surface energy.

In Figure 4B, a more slowly curing polymer, GAP-S, is used. Compared with Figure 4A, the same trends as described previously can be observed, only this time the effects are more dramatic. As in Figure 4A, the oxygen-plasma-treated sample has a peel strength that

increases steadily with time but the end value is much higher. For nitrogen plasma, the short 9-s treatment gives a very large increase in the peel strength (four times the strength of the untreated sample), but longer treatments give no significant difference from the untreated sample. The argon-treated sample also shows the same trend as in Figure 4A, a huge increase after a short treatment, then a lower, but still good, peel strength-after 2 min and very good strength after 6 min. These results relate to the surface energies in the same way as the GAP-F polymer in Figure 4A, because the trends are more or less the same, but at higher values. We believe that the higher peel strengths and more dramatic effects seen with this polymer can be explained by the diffusion theory of adhesion, because a lower rate of cure allows more and deeper penetration of components from the polymer into EPDM and thus would be expected to give better adhesion. It is also clear that diffusion alone cannot give good adhesion without consideration of the surface energies, or more precisely, that these two factors are interconnected.

For the peel samples with HTPE-based polymers shown in Figure 5, the same general trends are evident but the picture is not unambiguous. For the fastest curing polymer, in Figure 5A, the peel strength for the oxygen plasma treatment is low until 6 min, but then gives good peel strength. For nitrogen treatments, the trend is the same as for the GAP polymers. Short treatment gives medium to good peel strength around $0.7\,\mathrm{Nmm^{-1}}$; longer treatments reveal no improvement over the reference sample. With this polymer, the argon treatment again follows the same trend as the nitrogen treatment and does not give a higher value at 6 min, as with GAP-S polymer in Figure 3A. The HTPE polymers with lower rates of cure, however, do not give the same dramatic effects. With these polymers, the peel strength shows the same strong increase already with short plasma times but does not in the same way decrease with longer times. A slight decrease after 6 min of treatment may be observed for all the HTPE-M experiments in Figure 5B, but the uncertainties involved in these measurements do not invite a further discussion of the possible cause. The surface tension of the HTPE-based polymer is expected to be close to that of HTPE, $41.9\,\mathrm{mNm^{-1}}$ (polar component $11.1\,\mathrm{mNm^{-1}}$). This is lower than the GAP-based polymers, and the very high surface energies obtained by nitrogen and argon plasmas after longer times would be expected to be a disadvantage for the adhesion of the HTPE polymer, whereas oxygen plasma gives a surface more closely matched to this polymer. This is indeed seen to be the case for the HTPE-F polymer in Figure 5A but is not so for HTPE-M and HTPE-S in Figures 5B and C. For HTPE-F, the behavior of argon- and nitrogen-treated samples correlates well

with the surface energies at short times, as the surface energies then match the energy in the polymer well, but longer treatments give a larger difference because the EPDM surface then obtains polarity too high to match that of the polymer. When the HTPE polymers are formulated to give longer cure times, all peel strengths increase, as also observed for the GAP polymers. The influence of the exact magnitude of the surface energy then becomes smaller, as long as the polarity of the surface is considerably increased compared with the untreated insulation. Even for the untreated surfaces, the adhesion is improved by slower rate of cure and becomes even better with plasma treatment. It is therefore reasonable to conclude that the effect of diffusion is correlated to the degree of plasma treatment. There may be several reasons for this, both that the increased surface energy improves the penetration of the high surface energy polyol and that the higher surface roughness caused by plasma treatment also improves this diffusion and binding. We have shown earlier [6] that longer treatment times with plasma give a very rough surface. The slowest curing HTPE polymer, HTPE-S, is shown in Figure 5C; here only oxygen and nitrogen plasma treatments have been investigated. As expected, the peel strength of the untreated sample is higher than for the faster curing HTPE polymers, and also a further increase in the peel strengths with plasma treatment can be observed.

Generally, the uncertainties are greater for the HTPE polymer, probably due to many voids/bubbles that could be observed in the polymer after cross-linking. All peel strengths are also quite high, where the initiation of the failure will affect the measurement to a larger degree. Such flaws are present in the other polymer formulations as well, but to a lesser degree.

The HTPB polymer, shown in Figure 6, has a good peel strength prior to plasma treatment, but afterward the strength seriously deteriorated. The HTPB polymer is cured with IPDI-and thus cures very slowly, compared with all MDI-cured polymer formulations. The polymer also contains a larger excess of diisocyanate and thus cannot be directly compared with the MDI-based polymers. None-the-less, the results are very interesting. The surface tensions of the HTPB polymer is lower than the other polymers, *ca*. 38 mNm^{-1} (Table 3) with practically no polar component, and that of IPDI is more or less the same, 37 mNm^{-1}. It means that the surface energy of this polymer mixture is close to 38 mNm^{-1} and quite nonpolar. The untreated EPDM sample is also very nonpolar but has a lower total surface energy, *ca*. 25 mNm^{-1}. When the polar component of EPDM increases after plasma treatment, the peel strength decreases to low values, and this is observed for all three gases. The only exception from this trend

is with 6 min of oxygen plasma, which again gives a higher peel strength but still lower than the untreated value. The probable explanation for these observations is that when the polarity of the surface is low, the diffusion rates of the components, especially IPDI, are high enough during the available curing time to give relatively good adhesion to the untreated EPDM surface. The surface energy of the polymer is also more equal to that of the insulation, even if they are not exactly matched. However, after plasma treatment, the surface energy of EPDM increases considerably and the mismatch of surface energies becomes so great that adhesion is seriously hindered. Even here, some adhesion is possible due to diffusion.

The correlation between the surface energies and the observed peel strengths is quite interesting. Because plasma treatment not only chemically modifies the surface but also has other effects such as etching, this complicates matters, and it is therefore not surprising that especially after longer treatments, the correlation between surface energy and peel strength fails. In earlier work, we also found that most of the chemical modification occurs during the first seconds of plasma treatment, but etching of the surface is a more time-consuming process.

Depth of Penetration

The GAP-based polymer has an MDI/GAP weight ratio of approximately 0.42. We have earlier [4] found the self-diffusion coefficient for GAP at this ratio to be $3 \times 10^{-13} m^2 s^{-1}$, and for MDI $2 \times 10^{-12} m^2 s^{-1}$. In the EPDM insulation material we have earlier [5] measured the diffusion coefficient of MDI as $1.6 \times 10^{-14} m^2 s^{-1}$, whereas the diffusion coefficients of the polyols could not be measured by the applied method and were estimated to be at least $< 10^{-16} m^2 s^{-1}$. It may be useful to define a magnitude, "depth of penetration," as the distance $x = \sqrt{D_2 t}$, similar to the standard deviation of self-diffusion. At this distance, $c_2/C_0 = k/(1 + k\sqrt{D_2/D_1})\ \mathrm{erfc}(2) \approx 0.48k$ when $D_2 \ll D_1$. The depth of penetration increases proportionally to the square root of time, which is the usual dependency for irreversible diffusion. To further illustrate the penetration process, simulated concentration profiles for the GAP polymer across the interface are shown in Figure 7, using $1 \times 10^{-13} m^2 s^{-1}$ and $1 \times 10^{-16} m^2 s^{-1}$ as diffusion coefficient for GAP in the polymer and in the insulation, respectively, and with $k = 1$.

We see that the penetration process is quite slow, and even after 20 h, the depth of penetration is only *ca.* 3 μm, which is a very thin part of the insulation. However, it may be enough to obtain good adhesion. It may be expected that the solubility of the diffusing specie is lower in

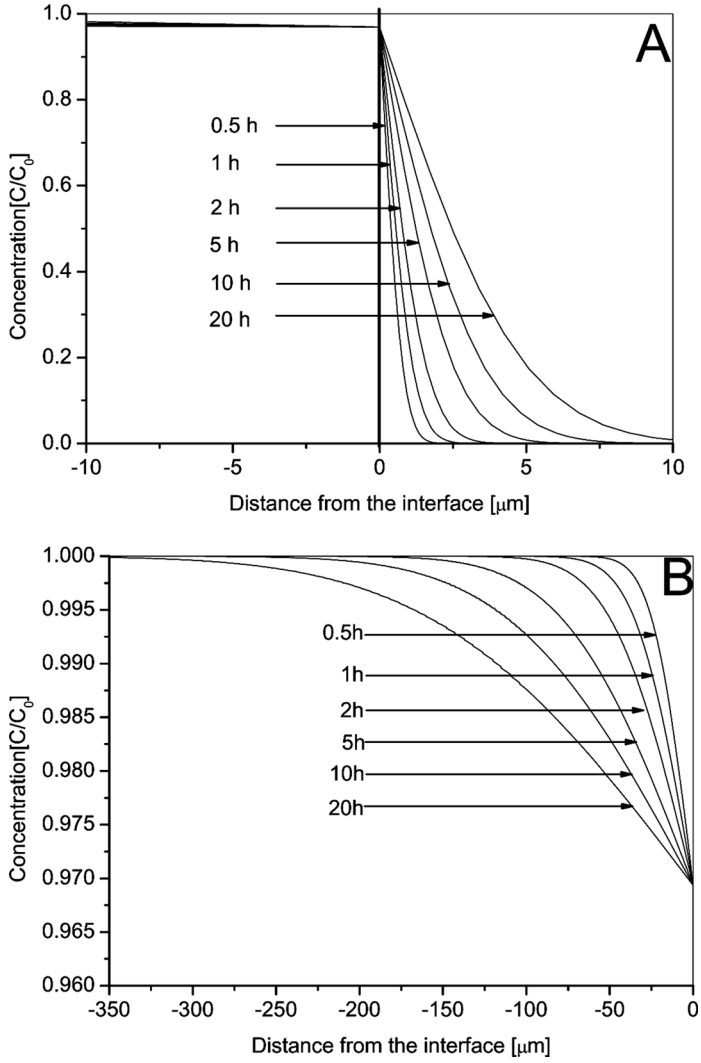

FIGURE 7 Diffusion of GAP from the polymer into the EPDM insulation, k = 1 (A), and composition of the polymer near the interface (B). In the simulation, the diffusion coefficient for GAP was $10^{-13}$and $10^{-16}$$m^2s^{-1}$ in the polymer and insulation, respectively.

the insulation material than in the polymer itself, and a value of k less than 1.0 should thus be used. The major effect of reducing the value of k is to reduce the total amount diffusing into the insulation material

(C_2/C_0 proportional to k), but the depth of penetration at a given time is the same as long as $D_2 \ll D_1$, as is the case here. On the other side, if k is increased as a result of plasma treatment, the amount of material diffused into the insulation will increase, even if the depth profile will stay the same as long as D_2 is not changed.

Because the amount of diffusing material decreases with lower solubility, it may explain a lower adhesion if the solubility is low, as more time is needed for the diffusion of a sufficient amount. It seems reasonable to assume that the more material that enters the insulation, the more links across the interface are possible. This may be one of the reasons for the better adhesion observed in the plasma-treated samples, because of the increased solubility. Also, it may explain why slower rates of cure give better adhesion for all samples. Because we have no really quantitative information on k or on the amount of polymer penetration needed to give good adhesion, it is difficult to calculate the exact effect of surface modification. Also, for the plasma-treated samples, the thickness of the modified layer is probably quite low, not more than a few nm. Therefore, it may be difficult to use these solubility considerations in a more quantitative fashion.

Figure 7B shows that the composition of the polymer near the interface changes. The level of change depends on k, but the depth of the influenced layer increases with time as shown. This gives rise to weaker cohesive strength in the polymer, because the ratio of polyol/diisocyanate changes from the optimum for a high molecular weight. However, we have in these experiments not observed any cohesively weakened polymer, probably because of an inherent excess of curing agent (the fastest diffusing specie) in the polymer.

Electron Microscopy

SEM was used to study 300-μm-thick cross-section sheets across the bonding surface. The samples selected for this study were an untreated sample with poor peel strength and some plasma-treated samples showing good peel strength to the polymers. The most interesting feature observed was in untreated samples, where missing adhesion in the form of small cracks could be observed at the polymer–insulation interface. An example with a GAP-F polymer is shown in Figure 8. This is the polymer that gives the lowest peel strength with the untreated insulation (Figure 4A). Because the polymer follows close to the insulation surface, it must be assumed that on this scale the polymer has wetted the insulation (there are no evident air bubbles), but because of low adhesion strength, and during either polymer curing (due to

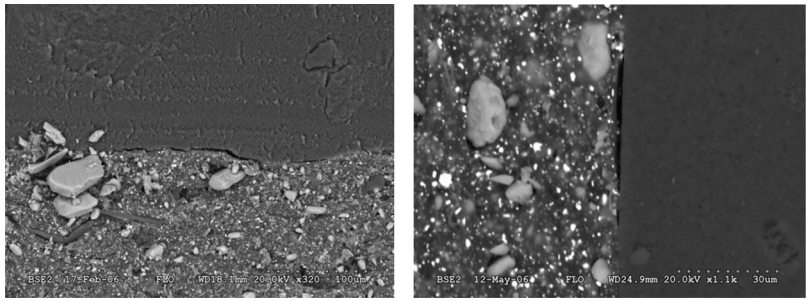

FIGURE 8 SEM picture of a cross-section of the bonding interface between untreated EPDM insulation and a GAP-F polymer, *ca*. 300 μm wide (A) and *ca*. 100 μm wide (B). Small cracks can be seen along the interface. EPDM is the phase that contains particles.

contraction) or by mechanical stresses due to sample preparation, a bonding failure occurs. Such cracks were not observed in the plasma-treated samples. In addition to these cracks, most samples showed some bubbles in the polymer, as seen in Figure 9. These bubbles where probably introduced by the process of either applying or of mixing the polymer. A variable amount of bubbles in all samples can explain much of the variation in the peel forces that has been observed between similar samples.

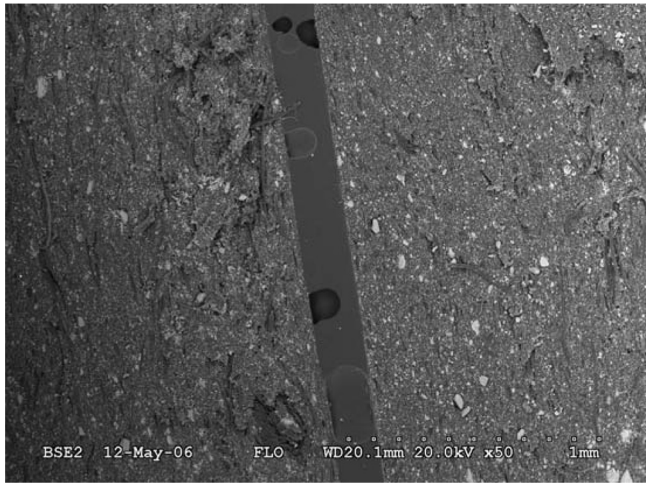

FIGURE 9 SEM picture showing common defects observed in the polymer layer, *ca*. 2.5 mm wide.

CONCLUSION

The use of plasma treatment can increase the total surface energy of EPDM/based rocket motor insulation materials from 27 to *ca*. 70 mNm^{-1}. The peel strength between the polar polymers based on GAP or HTPE and EPDM can be increased 1–10 times by use of plasma treatment. For a nonpolar polymer, HTPB, the peel strength is relatively good against an untreated surface but decreases after plasma treatment. We found that the matching of surface energies of the polymers and the plasma-treated EPDM surfaces was generally beneficial for the adhesive strength. We also found that the rate of cure of the polymer has an effect of the peel strength; the peel strength generally increased with a slower rate of cure. We can explain this by more and deeper diffusion of components from the polymer into the EPDM at a slower rate of cure. Additionally, there seems to be an interconnection between the diffusion process and the surface energies of the components as the surface energies are also a measure of the mutual solubility of the components.

ACKNOWLEDGMENT

We thank Jon Huse at Nammo Raufoss for general help with chemicals and discussions and Øivind Frigaard at the Norwegian Defence Logistics Organisation for operating the SEM. We also thank the Norwegian Defence Research Establishment and NAMMO Raufoss AS for financial support.

REFERENCES

[1] Comyn, J., *Adhesion Science* (RCS, Cambridge, 1997).
[2] Schreuder-Gibson, H. L., *Rubber World*. **203**, 34–44 (1990).
[3] Grythe, K. F., Master's Thesis, "Adhesion in solid propellant Rocket Motors," Chemical Engineering, NTNU, Trondheim, Norway, 2002.
[4] Grythe, K. F., Hansen, F. K., and Walderhaug, H, *Journal of Physical Chemistry B* **108**, 12404–12412 (2004).
[5] Grythe, K. F. and Hansen, F. K., *Journal of Applied Polymer Science* **103**(3), 1529–1538 (2007).
[6] Grythe, K. F. and Hansen, F. K., *Langmuir* **22**, 6109–6124 (2006).
[7] Fowkes, F. M., *Journal of Adhesion Science and Technology* **1**, 7–27 (1987).
[8] Morra, M., in *Encyclopedia of Surface and Colloid Science*, A. T. Hubbard (Ed.) (Marcel Dekker, New York, 2002).
[9] Johansson, B.-L., Larsson, A., Ocklind, A., and Ohrlund, A., *Journal of Applied Polymer Science* **86**, 2618–2625 (2002).
[10] Kaminska, A., Kaczmarek, H., and Kowalonek, J., *European Polymer Journal* **38**, 1915–1919 (2002).

[11] Hegemann, D., Brunner, H., and Oehr, C., *Nuclear Instruments and Methods in Physics Research, Section B: Beam Interactions with Materials and Atoms* **208**, 281–286 (2003).
[12] Nihlstrand, A., Hjertberg, T., Schreiber, H. P., and Klemberg-Sapieha, J. E., *Journal of Adhesion Science and Technology* **10**, 651–675 (1996).
[13] Beake, B. D., Ling, J. S. G., and Leggett, G. J., *Journal of Materials Chemistry* **8**, 2845–2854 (1998).
[14] Clouet, F. and Shi, M. K., *Journal of Applied Polymer Science* **46**, 1955–1966 (1992).
[15] Landete-Ruiz, M. D., Martinez-Diez, J. A., Rodriguez-Perez, M. A., De Saja, J. A., and Martin-Martinez, J. M., *Journal of Adhesion Science and Technology* **16**, 1073–1101 (2002).
[16] Osterhold, M. and Armbruster, K., *Progress in Organic Coatings* **33**, 197–201 (1998).
[17] Liston, E. M., Martinu, L., and Wertheimer, M. R., *Journal of Adhesion Science and Technology* **7**, 1091–1127 (1993).
[18] Carrino, L., Polini, W., and Sorrentino, L., *Journal of Materials Processing Technology* **153–154**, 519–525 (2004).
[19] Foerch, R., Izawa, J., McIntyre, N. S., and Hunter, D. H., *Journal of Applied Polymer Science: Applied Polymer Symposium* **46**, 415–437 (1990).
[20] Paynter, R. W., *Surface and Interface Analysis* **33**, 14–22 (2002).
[21] Dyckerhoff, G. A. and Sell, R. J., *Angew. Makromol. Chem.* **21**, 169 (1972).
[22] Iyengar, Y. and Erickson, D. E., *J. Appl. Polym. Sci.* **11**, 2311 (1967).
[23] Luciani, A., Champagne, M. F., and Utracki, L. A., *Polym. Networks Blends* **6**, 41–50 (1996).
[24] Brewis, D. M., *Plasma and Other Pretreatments to Enhance the Adhesion to Polymers* (Antibes, France, 1999), pp. 157–161.
[25] Dahm, R. H., Brewis, D. M., Mathieson, I., and Tegg, J. L., *RubberChem 2002, International Rubber Chemicals, Compounding and Mixing Conference*, Munich (Rapra Techonology Ltd., Shrewsbury, UK, 2002), pp. 75–83.
[26] N. N., Huels Chemische Werke AG, 1975.
[27] Kondyurin, A. V., *Journal of Applied Polymer Science* **48**, 1417–1423 (1993).
[28] Wheale, S. H., Badyal, J. P. S., Bech, J., and Nilsson, N. H., *Polymer Surfaces and Interfaces III*, Durham, UK (Wiley, Chichester, UK, 1999), pp. 285–297.
[29] Husein, I. F., Chan, C., and Chu, P. K., *Journal of Materials Science Letters* **21**, 1611–1614 (2002).
[30] Osterhold, M. and Armbruster, K., *Macromolecular Symposia* **126**, 295–306 (1998).
[31] Konar, J., Kole, S., Avasthi, B. N., and Bhowmick, A. K., *Journal of Applied Polymer Science* **61**, 501–506 (1996).
[32] Wu, S., *Polymer Interface and Adhesion* (Marcell Dekker, New York, 1982).
[33] Pocius, A. V., *Adhesion and Adhesives Technology: An Introduction* (Hanser, München, 2002).
[34] Packham, D. E., in *Handbook of Adhesion*, D. E. Packham (Ed.) (Longman Scientific & Technical, Essex, 1992).
[35] Chin, J. W. and Wightman, J. P., *J. Adhesion* **41**, 23–34 (1992).
[36] Hansen, F. K., *J.Colloid Interface Sci.* **160**, 209–217 (1993).
[37] Owens D. K. and Wendt, R. C., *Journal of Applied Polymer Science* **13**, 1741–1747 (1969).
[38] Kaelble, D. H., *Journal of Adhesion* **2**, 66–81 (1970).
[39] Kaelble, D. H., *Physical Chemistry of Adhesion* (Wiley, New York, 1971), Chaps. 5, 13.

[40] Dalet, P., Papon, E., and Villenave, J. J., *Journal of Adhesion Science and Technology* **13**, 857–870 (1999).
[41] Kwok, D. Y., Li, D., and Neumann, A. W., *Langmuir* **10**, 1323–1328 (1994).
[42] Crank, J., *The Mathematics of Diffusion* (Clarendon Press, Oxford, 1975).
[43] Tyrell, H. J. V. and Harris, K. R., *Diffusion in Liquids* (Butterworths, London, 1984).